Asian Journal of Chemistry; Vol. 25, No. 2 (2013), 739-744

ASIAN JOURNAL OF CHEMISTRY

http://dx.doi.org/10.14233/ajchem.2013.12824

Controlled Synthesis and Photocatalytic Activity of TiO_2 Nanoparticles by a Novel Gel-Network Precipitation Method

YINGLING WANG[1,2,*], YOUHAI XIE[1], JIANMEI YUAN[2] and GUOGUANG LIU[1,*]

[1]School of Chemistry and Environmental Science, Henan Normal University, Key Laboratory for Yellow River and Huaihe River Water Environment and Pollution Control, Ministry of Education, Xinxiang 453007, Henan Province, P.R China
[2]School of Basic Medicine, Xinxiang Medical University, Xinxiang 453003, Henan Province, P.R. China

*Corresponding author: Fax: +86 373 3328507; Tel: +86 373 3326211; E-mail: wangyingling2004@163.com

(*Received*: 8 October 2011; *Accepted*: 16 August 2012) AJC-11967

Using gelatin as a based template, monodispersed spherical TiO_2 nanoparticles were successfully synthesized by a novel gel-network precipitation(GNP) method. The well-crystallized anatase TiO_2 have narrow size distribution of 20 nm. The aim of our work was to investigate the influence of reaction conditions on the formation process, structure and photocatalytic activity of the samples. TG-DTA, XRD, TEM, FT-IR, UV-VIS DRS and HPLC were used to characterize the samples. The results showed that the particle sizes were related to the network structure of gelatin, not only could the crystalline phases and sizes of nanoparticles be controlled, but the aggregation and agglomeration could be prevented by gel-network. The products have smaller particle size and better homogeneity. To examine the photocatalytic activity of the samples, the photocatalyic degradation rate of rhodamine B (RB) was investigated in the suspension of TiO_2 nanoparticles. It was found that well-crystallized anatase TiO_2 (ψ = 8 %) calcined at 650 ºC for 2 h nearly induced complete degradation of rhodamine B. Relationship between degradation rate of rhodamine B and grain sizes of TiO_2 nanoparticles under different gelatin concentration and calcination temperature were given. The enhancing of the photocatalytic activity was attributed to the increase of phase transformation temperature and uniformity of the particle sizes.

Key Words: Nanocrystalline TiO_2, Gel-network precipitation method, Photocatalytic activity, Rhodamine B.

INTRODUCTION

Chemical reactions carried out under light illumination with inorganic semiconductors presence are the subject of intensive investigation during last 20-25 years[1-4]. These reactions called photocatalytic processes are one of advanced oxidation technologies[5-7]. Semiconductor photocatalysis is an alternative method for conventional water treatment technologies. Water contamination is caused by various sources such as industrial effluents, agricultural runoff and chemical spills. Industrial effluents contain several non-biodegradable substrates that can be harmful to the environment[8]. One major source of these effluents is the waste arisings from the industrial processes, which utilize dyes to colour paper, plastic and natural and artificial fibres[9]. A substantial amount of dyestuff is lost during the dyeing process in the textile industry, which poses a major problem for the industry as well as a threat to the environment[10-13]. Decolourization of dye effluents has therefore acquired increasing attention. During the past two decades, photocatalytic processes involving TiO_2 semiconductor particles under UV light illumination have been shown to be potentially advantageous and useful in the treatment of wastewater pollutants.

TiO_2 is the most often used photocatalyst due to its considerable photocatalytic activity, high stability, non-environmental impact and low cost. Recently, many different methods have been used in preparing TiO_2 nanoparticles. Among the various methods, the thermal treatment of precursors obtained by sol-gel[14,15], precipitating of $TiCl_4$[16] and $Ti(SO_4)_2$[17] have been widely investigated due to the benefits of easily controlled process. Conventionally, there are three well-known crystalline types of TiO_2 *e.g.*, anatase, rutile and brookite. The phase transition of A→R-TiO_2, which occurs during calcination[18], gives rise to transformed rutile powder, which has undergone considerable aggregation and grain growth[19]. The above characteristics are detrimental to the formation of TiO_2 nanoparticles. The literature concerning phase formation and influence on photocatalytic activity in these powders, however, contains conflicting results. Rhodamine B ($C_{28}H_{31}N_2O_3Cl$) is one of the most important xanthene dyes and hard to be degraded, the titania-assisted photodegradation of rhodamine B solution has been well studied[20-24], so we employed the photocatalytic degradation of rhodamine B as a model reaction to evaluate the photocatalytic activity of the TiO_2 samples.

In this paper, a novel controlled synthesis technique for TiO_2 nanoparticles using a gel-network precipitation (GNP) method was reported, the as-synthesized samples were also characterized by TG-DTA, XRD, TEM, FT-IR, UV-VIS DRS and HPLC. Moreover, the influence of gelatin concentration (*i.e.*, the weight ratio of gelatin to gel-mixture, which is hereafter referred to as ψ) and calcination temperature on the crystalline phases, crystallites sizes and photocatalytic activity of the TiO_2 nanoparticles were studied. It is hoped that this paper can give more significant results for preparation and characterization of an efficient photocatalyst with high activity.

EXPERIMENTAL

TiO_2 Nanoparticles synthesis: The TiO_2 samples consisting of 20 nm diameter anatase nanoparticles were synthesized by a novel gel-network precipitation method with gelatin as a based template. $Ti(SO_4)_2$, $NH_3{\cdot}H_2O$ and gelatin were used as starting materials. Gelatin was weighed at different weight ratio (ψ) such as 4, 5, 8, 11, 14 and 17 %, then it was directly dissolved in the 100 mL 0.5 mol L^{-1} $Ti(SO_4)_2$ solution with vigorous stirring at 70 ºC in water bath and continuously stirred for 0.5 h at 70 ºC, which make them almost as homogeneous mixture. Then the mixture was cooled to 5 ºC, turning to a yellowish transparent gel. The gel-mixture was cut into small pieces and then soaked in 150 mL, 4 mol L^{-1} $NH_3{\cdot}H_2O$ solution for 24 h at 5 ºC. The hydroxides were precipitated in the gel-network. The gel was washed three times with deionized water (70 ºC) to remove vitriolic ion and residual ammonia at 70 ºC in water bath and then dried at 105 ºC. The dried powder obtained is termed as the "precursor". After an intermediate grinding, the powder was subsequently calcined at various temperature from 400-900 ºC for 2 h in a muffle furnace in air, producting fine TiO_2 powder. The obtained photocatalyst was ground with an agate mortar before use.

Differential thermal analysis (DTA) and thermogravimetric (TG) analysis were carried out with a Shimadzu DT-40 analyzer, at a rate of 10 ºC/min under static air conditions in the temperature range 20-800 ºC, to analyze the decomposition reaction and phase transformation of the precursor. The crystalline phase of the TiO_2 nanoparticles was analyzed by XRD with a CuK_α radiation at 40 kV with a graphite monochromator and scans at 3º/min (2θ) with a Bruker D8 Advance X-ray diffractometer. The particle size and morphology of the samples were examined using a 200 CX transmission electron microscope (TEM, Model 200CX, Jeol, Tokyo, Japan). To investigate the changes in the local structure of TiO_2, FT-IR spectra were monitored by Bio-Rad FTS-40 (USA). The UV-VIS DRS spectra were obtained by U-4100 spectrophotometer. The BET surface areas were determined from nitrogen adsorption data (Micromeritics, ASAP-2010).

Photocatalytic activity: All the photocatalysis experiments were performed in a 350 mL hollow cylindrical photoreactor equipment (SGY-1, Nanjing STO Co. Ltd.) equipped with a quartz water jacket. The set-up is displayed as in Fig. 1. A 300 W high-pressure mercury lamp with a primary wavelength distribution at approximately 365 nm was positioned in the inner part of the photoreactor and cooling water circulated through the quartz jacket surrounding the lamp. The average light intensity in the solution was about 8 mW cm^{-2}. Batch experiments were conducted at 25 ± 2ºC.

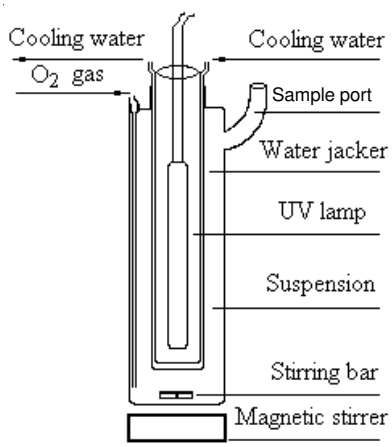

Fig. 1. Scheme of the photoreactor

Before the exposure experiments, the experimental solution was prepared as follows: 350 mL rhodamine B solution with the concentration of 100 mg L^{-1} was piped into a brown flask and 0.35 g photocatalyst was added into it under the shaking in an ultrasonicator for 10 min. Then the solution was transferred to the photoreactor, the O_2 was aerated to the solution at a rate of 200 mL min^{-1} and then the light was turned on. The parallel aliquots of 5 mL were taken from the sample port at various intervals for analysis after removal of the catalyst by centrifugation at 4000 rpm for 20 min. The absorbance of residual rhodamine B was detected by HPLC and the degradation rate of rhodamine B was calculated.

RESULTS AND DISCUSSION

TG-DTA analysis of precursor: Fig. 2 showed the TG-DTA curves of the precursor (ψ = 8 %). It could be found that there were three main stages during the weight loss process of precursor from the TG curve. The first weight loss (*ca.* 8.1 %) was observed at the temperature range from 52-273 ºC, which mainly resulted from the desorption or release of absorbed water and some organic matters in the precursor, this loss step was accompanied by a wide endothermic peak in DTA curve; the second stage was that the rate of weight loss is *ca.* 13.9 % between 273 and 429 ºC, an exothermic peak appeared around 332 ºC from the DTA curve, possibly resulting from the combustion decomposition of the residual gelatin and the phase transition of TiO_2 from amorphous to anatase; the third weight loss (*ca.* 11.6 %) occurred from 429-544 ºC, the strong exothermic peak was also observed around 497 ºC, corresponding to the completion of anatase crystallization, C and CO combustion process of the organic matters simultaneously. There were no exothermic peaks above 554 ºC, suggesting that pure and well-crystallized TiO_2 has formed.

XRD analysis: XRD is usually used for crystal phase identification and estimation of the anatase to rutile ratio as well as crystallite size of each phase present. The XRD peaks at 2θ = 25.25(101) and 48.0º in the spectrum of TiO_2 are easily identified as the crystal of anatase form, whereas the XRD peaks at 2θ = 27.42(110) and 54.5º are easily identified as the crystal of rutile form[8,18]. The crystallite size can also be deter-

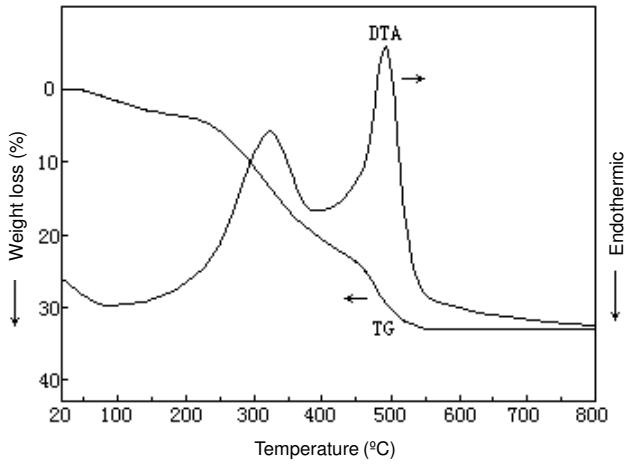

Fig. 2. TG-DTA analyses of precursor

mined from the broadening of corresponding X-ray spectral peaks by Scherrer formula: $L = k\lambda/(\beta \cos \theta)$, where L is the crystallite size, λ the wavelength of the X-ray radiation (CuK_α = 0.15418 nm), K usually taken as 0.89 and β is the line width at half-maximum height[25]. This is a generally accepted method to estimate the mean crystallite size of nanoparticle.

Fig. 3 showed the XRD patterns of the TiO_2 samples (ψ = 8 %) made from the precursor calcined for 2 h at the temperature range from 400-900 ºC, which demonstrated the effects of calcination temperature on phase composition and size of the samples. Obviously, the amorphous phase crystallized to the anatase structure at temperature of 400 ºC, when the TiO_2 was heated up to 550 ºC and above, the products became anatase, this was in good agreement with the results of TG-DTA. However, the phase transition of A→R-TiO_2 did not occur when the calcination temperature was 750 ºC. When the TiO_2 was heated up to 800 ºC, the weaker phase transformation from anatase to rutile began to appear. In addition, the XRD peaks of anatase phase became sharper and stronger with the increasing calcination temperature, indicating that the crystallite of anatase TiO_2 was perfectly formed. The XRD data also showed the crystal size of TiO_2 increased from 8.4-50.9 nm by above Scherrer's formula as the temperature was increased from 400-900 ºC. Consequently, the crystalline phases and sizes of TiO_2 nanoparticles synthesized by gel-network precipitation method can be controlled during calcination process which shifted the A→R phase transformation to a higher temperature.

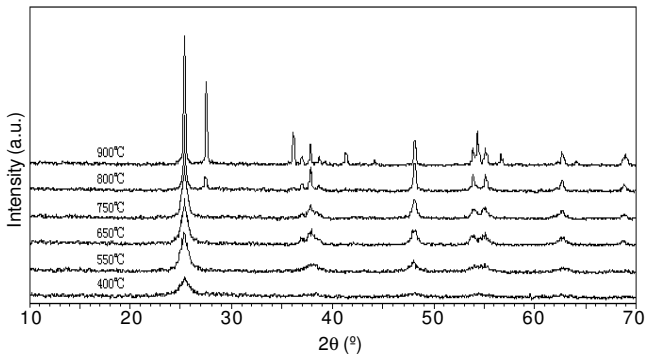

Fig. 3. XRD patterns of the samples calcined at different temperatures

TEM analysis: The particle dimensions and morphology of the TiO_2 sample (ψ = 8 %) were carried out through TEM technique. Fig. 4(a,b) showed TEM photographs of TiO_2 nanoparticles synthesized by calcined the precursor at 650 ºC for 2 h. It could be seen that TiO_2 nanoparticles were nearly spherical with the average size of *ca.* 20 nm, which was in good accordance with XRD results. For the comparison, the specific surface area of TiO_2 samples and degussa P25 were acquire under the BET adsorption. The sample (ψ = 8 %) calcined at 650 ºC possessed higher specific surface area (102.5 $m^2 g^{-1}$ according to BET) than Degussa P25 (S_{BET} = 50 $m^2 g^{-1}$), which increased the adsorption of the reactant and light and thus enhance the photocatalytic activity.

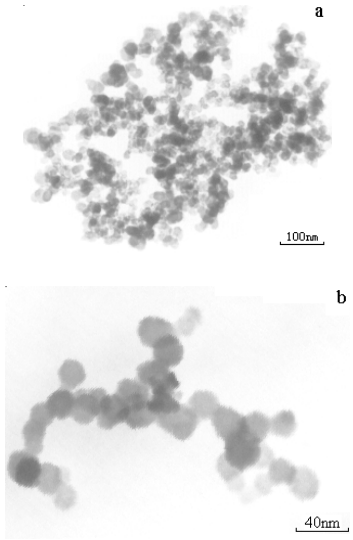

Fig. 4. TEM photographs of the sample calcined at 650 ºC

Effect of reaction conditions on particle size: In this paper, a novel gel-network precipitation method for the preparation of TiO_2 nanoparticles was constructed by combining sol-gel technique precipitation process. $Ti(SO_4)_2$ were first immersed into the gelatin solution to assemble three-dimensional gel-network structure and Ti(IV) was immobilized by decreasing temperature, then ammonia (4.0 mol L^{-1}) were chemisorbed onto the gelatin group of the gel-network. The gel-network is similar to "nanometer reactor fabricated" by microemulsion and macromolecule-emulsion solution which can prevent the aggregation and agglomeration of nanoparticles. Fig. 5 shows the effect of preparation condition on particle sizes of TiO_2 nanoparticles by changing gelatin concentration and calcinations temperature. Fig. 5 showed the particle sizes of the sample (650 ºC, 2 h) decrease from 38.7-11.1 nm with increasing gelatin concentration in the range of 4-17 %. Meanwhile, it can also be seen that the particle sizes vary from 9.6-50.9 nm in the range 400-900 ºC. Thus, fabrication procedure of TiO_2 nanoparticles were optimized with respect to the reaction conditions.

FT-IR spectra analysis: Fig. 6 showed the FT-IR spectra of the precursor and TiO_2 samples (ψ = 8 %) calcined at different temperature in the range 4000-400 cm^{-1}, respectively. The precursor FT-IR spectra showed the broad absorption region at approximately 3500-3200 $cm^{-1}$was attributed to the O-H stretching vibration and the band at 1641 cm^{-1} was attributed

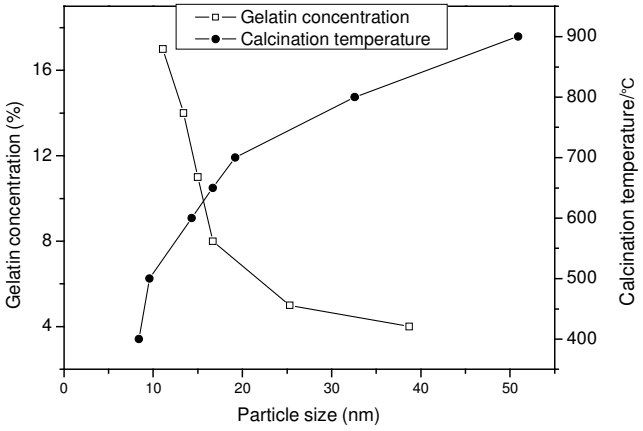

Fig. 5. Particle sizes as functions of reaction conditions

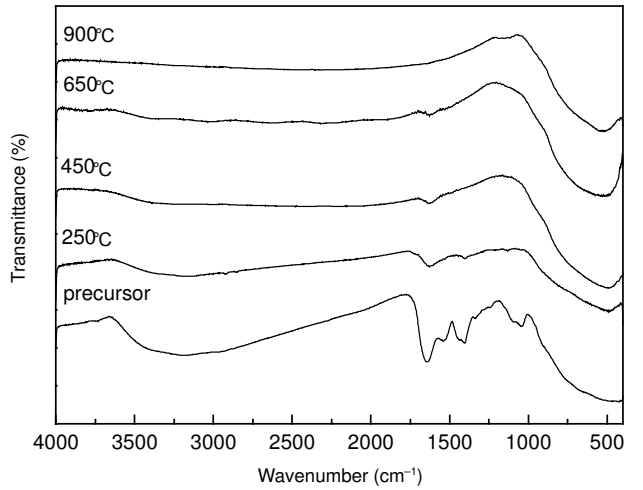

Fig. 6. FT-IR spectra of precursor and the samples calcined at different temperatures

to the O-H bending vibration of the physically absorbed water[26,27]. A second typical absorption band at about 3145, 1404 cm^{-1} were assigned to the stretching and bending vibration of primary ammonia[28,29]. The Ti-O-C absorption peak occurred at 1039 cm^{-1}.

In the FT-IR spectrum of the TiO_2 samples, both the O-H bands decreased intensity with increasing calcination temperature, showing that the hydroxy groups were removed gradually from the precursor. The disappearance of the characteristic bands NH_4^+ and Ti-O-C at 450 ºC revealed that anatase TiO_2 has already been formed. In addition, there's only one significant spectroscopic band at around 500 cm^{-1}. This is the characteristic bands of TiO_2 and the band can be clearly observed to shift towards higher wavenumber with increasing temperature from *ca.* 453 cm^{-1} after calcined at 250 ºC to 544 cm^{-1} after calcined at 900 ºC. These position variation could be possibly related to phase separation and TiO_2 crystallization together with quantum size effect.

UV-VIS DRS spectra analysis: Fig. 7 showed UV-VIS DRS spectra of P25, as well as the corresponding spectra of the TiO_2 sample (ψ = 8 %, 650 ºC). The UV-VIS DRS spectra of TiO_2 sample revealed strong wide absorption bands in the ultraviolet region of 300-380 nm and significant visible light absorption. Absorption edges for TiO_2 sample synthesized by gel-network precipitation shift to longer wavelength *ca.* 400 nm

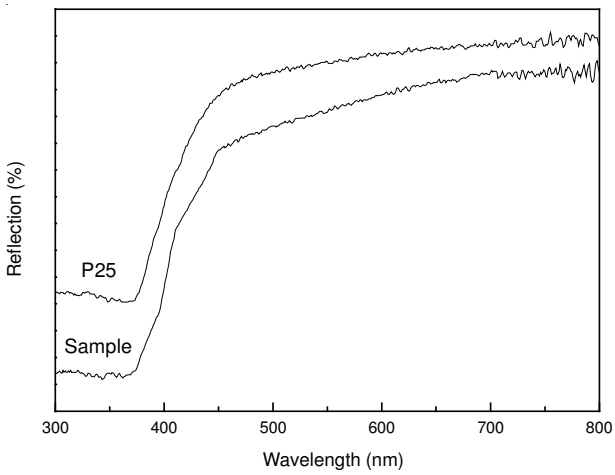

Fig. 7. UV-VIS DRS spectra of P25 and the sample calcined at 650 ºC

compared to the absorption threshold of P25, indicating that gap energies for TiO_2 sample the fact can be attributed to stronger quantum effect on the anatase grains. It means that for TiO_2 nanopowders the yields of the photogenerated electron-hole pair would increase, because the photoreaction needs photons with lower energy to band gap broadening and relatively the intensity of incident photons than can initiate the TiO_2 photoreaction increase. It's favorable for the TiO_2 photocatalysis.

Photodegradation of rhodamine B aqueous solution: Fig. 8 shown the absorbance spectra of the rhodamine B aqueous solution (C_0 = 100 mg L^{-1}) in the presence of the TiO_2 sample (gelatin 8 %, 650 ºC, 2 h) use as photocatalyst during the irradiation, with wavelength covering from 400-600 nm. With the increasing irradiation time up to 1 h, the intensity of the maximum peak located near 554 nm decreased gradually to a value near zero. No remarkable peak shift was observed. To confirm that TiO_2 sample induce complete photodegradation of rhodamine B, 98 % degradation ratio and 96 % mineralization ratio of rhodamine B were observed using HPLC and TOC, respectively. Under the irradiation of the high-pressure mercury lamp, TiO_2 sample can absorb effectively ultraviolet light and visible light, creating highly reaction electron and hole pairs. The holes, together with hydroxyl radicals and oxygen species, nearly completely oxidize the rhodamine B in aqueous solution to CO_2, H_2O and simple inorganic small molecule.

Effect of gelatin concentrations on photocatalytic activity of TiO_2: Degradation of rhodamine B (100 mg L^{-1}) under the catalysis of TiO_2 (gel-network precipitation) nanoparticles were investigated in the presence of O_2 at the rate of 200 mL min^{-1}. Meanwhile the degradation of rhodamine B with TiO_2 nanoparticles in the darkness and the direct photolysis of rhodamine B were also investigated in the same condition. The results are shown in Fig. 9. No obvious degradation of rhodamine B was observed in the darkness. When illuminated with UV light, 37 % degradation of rhodamine B within 1 h was observed. However, the degradation of rhodamine B was greatly accelerated in the illuminated TiO_2 suspensions. The concentrations of gelatin in gel-network precipitation methods have significantly influence on the photocatalytic activity of TiO_2. Complete degradation of rhodamine B

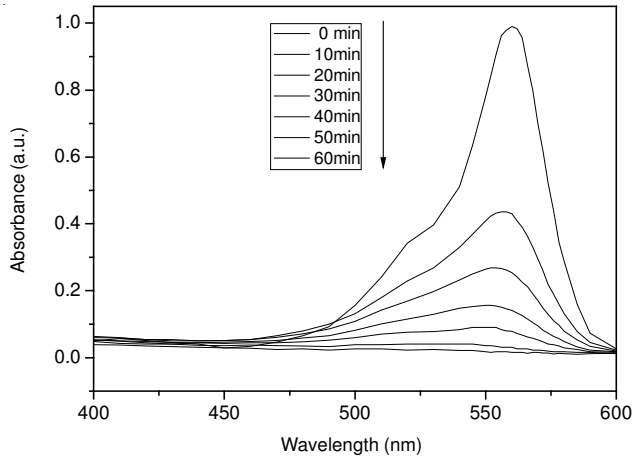

Fig. 8. Absorbance spectra of the aqueous solution of rhodamine B after irradiation for different durations

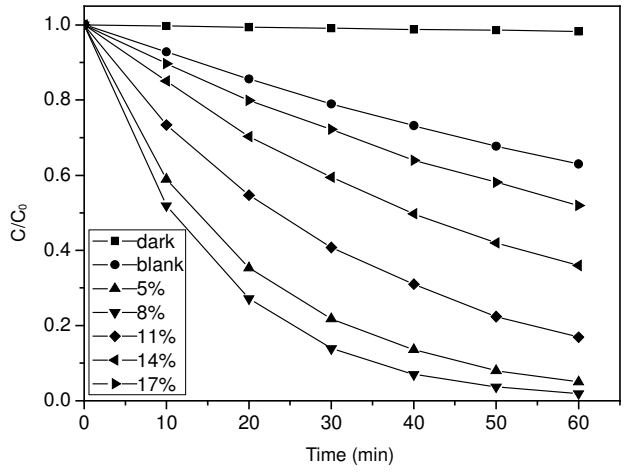

(a)

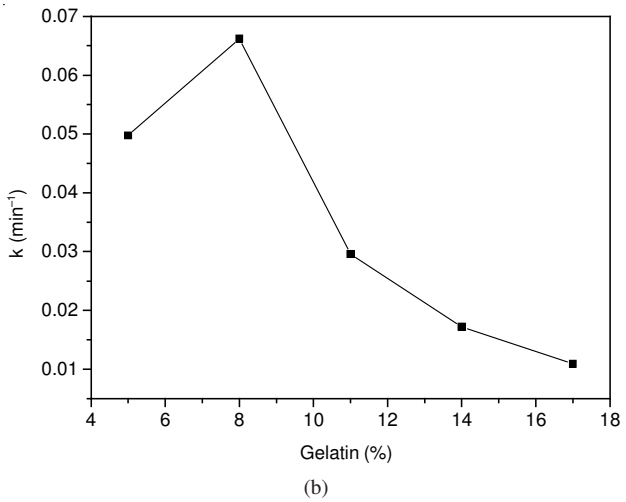

(b)

Fig. 9. Relation between degradation ratio of rhodamine B and gelatin concentration (ψ)

occurred under the photocatalysis of TiO_2 (gel-network precipitation) within 1 h. Our experiments expressed that the degradation of rhodamine B TiO_2 was an apparent first-order[30,31]. The apparent rate constants (k_{obs}) of rhodamine B under the catalysis of TiO_2 are 0.04976, 0.06618, 0.02955, 0.01723 and 0.01092 min^{-1}. The k_{obs} is 0.06618 min^{-1} for TiO_2 (gelatin 8 %), which is more than twice that of pure TiO_2, indicating that Zn^{2+} doping in the solid phase reaction methods is an effective way to enhance the photocatalytic activity of TiO_2.

Effect of calcination temperature on photocatalytic activity of TiO_2: In present experiment, TiO_2 nanoparticles were synthesized by calcined from 500-900 ºC and their photocatalytic activities for rhodamine B degradation are shown in Fig. 10. The k_{obs} is 0.0231, 0.05014, 0.06618, 0.04436, 0.01528 and 0.00869 min^{-1} for TiO_2 calcined at 500, 600, 650, 700, 800 and 900 ºC, respectively. Although the photocatalyst calcined at 650 ºC has a larger particle size (20 nm), it showed higher efficiency than that calcined at 500 and 600 ºC in rhodamine B degradation. The TiO_2 only existed as anatase, but when it was calcined at 800 ºC, TiO_2 existed with partly anatase and rutile. TiO_2 tranrformed mostly into rutile at 900 ºC.

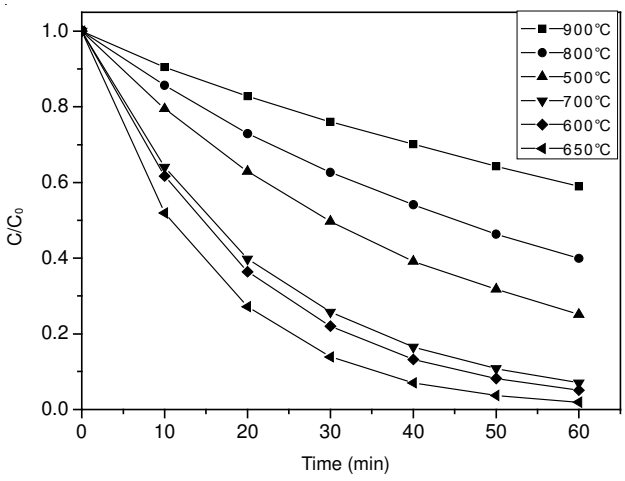

(a)

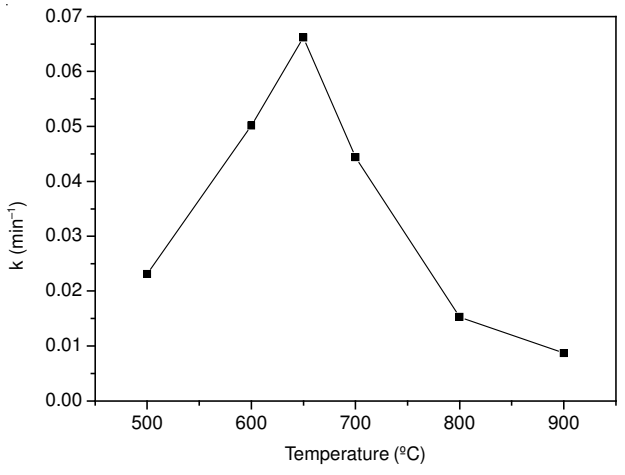

(b)

Fig. 10. Relation between degradation rate of rhodamine B and calcination temperature

Conclusion

Using gelatin as a based template, a novel gel-network precipitation method has been successfully synthesized nanocrystalline TiO_2 photocatalysts. The well-crystallized anatase products are spherical particles with narrow size

distribution of 20 nm. Gelatin concentration and calcination temperature have obvious influence on the size, sturcture and activities of the samples, not only can the crystalline phases and sizes of nanoparticles be controlled, but also the aggregation and agglomeration can be prevented through gel-network. To the photocatalytic activity of these materials, the photocatalytic degradation rate of rhodamine B in water is invistigated. It is found that the sample (gelatin 8 %, 650 ºC, 2 h) can nearly completely degradate rhodamine B. The high photocatalytic activity of TiO_2 is attributed to the increase of phase transformation temperature and uniformity of the particle size, obtained through the gel-network structure. Gel-network precipitation method is the first combination of sol-gel technique and precipitation process. Comparing with other methods, gel-network precipitation is a simple, quick and inexpensive way to make higher-active TiO_2. It's provided a kind of effective method for preparation of other nanometer powders.

ACKNOWLEDGEMENTS

The authors acknowledged the financial support by Henan Research Program of Foundation and Advanced Technology (No. 112300410104; 112102310656).

REFERENCES

1. M. Schiavello, Photocatalysis and Environment, Kluwer Academic Publishers, Dordrecht (1988).
2. D.F. Ollis and H. Al-Ekabi, Photocatalytic Purification and Treatment of Water and Air, Amsterdam (1993).
3. M.R. Hoffmann, S.T. Martin, W. Choi and D.W. Bahnemenn, *Chem. Rev*., **95**, 69 (1995).
4. D.M. Blake, Bibliography of Work on the Photocatalytic Removal of Hazardous Compounds from Water and Air, NREL/TP-430-22197, Golden Co. (1997).
5. J. Tseng and C.P. Huang, In: Proceedings of the 1st International Symposium on Chemical Oxidation Technologies for the Nineties, Vanderbilt University, Nashville, TN, **1**, 262 (1991).
6. J.M. Herrmann, *Catal. Today*, **53**, 115 (1999).
7. R. Andreozzi, V. Caprio, A. Insola and R. Marotta, *Catal. Today*, **53**, 51 (1999).
8. O. Ligrini, E. Oliveros and A. Braun, *Chem. Rev*., **93**, 671 (1993).
9. H. Zollinger, In eds.: H.F. Eblel and C.D. Brenzinger, Colour Chemistry, New York: VCH, edn. 1 (1987).
10. C.E. Searle, Chemical Carcinogenesis, ACS Monograph, Washington, DC: American Chemical Society (1976).
11. C.T. Helmes, C.C. Sigman, Z.A. Fund, M.K. Thompson, M.K. Voeltz and M. Makie, *J. Environ. Sci. Health A*, **19**, 97 (1984).
12. M. Boeninger, Carcinogenicity and Metabolism of Azo Dyes, Especially those Derived from Benzidine, DHHS (NIOSH), **80**, 119 (1980).
13. J.J. Roxon, A.J. Ryan and S.E. Wright, *Food Cosmet. Toxicol.*, **5**, 367 (1967).
14. F. Cot, A. Larbot, G. Nabias and L. Cot, *J. Eur. Ceram. Soc.*, **18**, 2175 (1998).
15. J. Yang, S. Mei and J.M.F. Ferreira, *J. Am. Ceram. Soc*., **84**, 1696 (2001).
16. Y. Zheng, E. Shi, Z. Chen, W. Li and X. Hu, *J. Mater. Chem*., **11**, 1547 (2001).
17. H.K. Park, Y.T. Moon and D.K. Kim, *J. Am. Ceram. Soc*., **79**, 2727 (1996).
18. K.J.D. MacKenzie, *Trans. J. Br. Ceram. Soc*., **74**, 29 (1975).
19. A. Gribb and J.F. Banfield, *Am. Min*., **82**, 717 (1997).
20. Y. Ma and J.N. Yao, *Chemosphere*, **38**, 2407 (1999).
21. Y. Ma and J.N. Yao, *J. Photochem. Photobiol. A: Chem*., **116**, 167 (1998).
22. T.X. Wu, G.M. Liu, J.C. Zhao, Hidaka and N. Serpone, *J. Phys. Chem. B*, **102**, 5845 (1998).
23. F.L. Zhang, J.C. Zhao, L. Zang, T. Shen, H. Hidaka, E. Pelizzetti and N. Serpone, *J. Mol. Catal. A: Chem*., **120**, 173 (1997).
24. T. Watanabe, T. Takizawa and K. Honda, *J. Phys. Chem*., **81**, 1845 (1977).
25. H. Ogawa and A. Abe, *J. Electrochem. Soc*., **128**, 685 (1981).
26. J.F. Rabek, Photo Stabilization of Polymers, Principles and Applications, London, p. 182 (1990).
27. L.A. Phillips and G.B. Raupp, *J. Mol. Catal*., **77**, 297 (1992).
28. G. Ramis, G. Busca, V. Lorenzelli and P. Forzatti, *Appl. Catal*., **64**, 243 (1990).
29. A.A. Tsyganenko, D.V. Pozdnyakov and V.N. Filimonov, *J. Mol. Struct*., **29**, 299 (1975).
30. G.G. Liu, X.Z. Zhang, Y.J. Xu, X.S. Niu and X.J. Ding, *Chemosphere*, **55**, 1287 (2004).
31. G.G. Liu, X.Z. Zhang, Y.J. Xu, X.S. Niu, L.Q. Zheng and X.J. Ding, *Chemosphere*, **59**, 1367 (2005).